

Evaluation of Neel temperatures from fully self-consistent broken-symmetry GW and high-temperature expansion: application to cubic transition-metal oxides

Pavel Pokhilko¹ and Dominika Zgid^{1,2}

¹*Department of Chemistry, University of Michigan, Ann Arbor, Michigan 48109, USA*

²*Department of Physics, University of Michigan, Ann Arbor, Michigan 48109, USA*

Using fully self-consistent thermal broken-symmetry GW we construct effective magnetic Heisenberg Hamiltonians for a series of transition metal oxides (NiO, CoO, FeO, MnO), capturing a rigorous but condensed description of the magnetic states. Then applying high-temperature expansion, we find the decomposition coefficients for spin susceptibility and specific heat. The radius of convergence of the found series determine the Neel temperature. The NiO, CoO, and FeO contain a small ferromagnetic interaction between the nearest neighbors (NN) and the dominant antiferromagnetic interaction between the next-nearest neighbors (NNN). For them the derived Neel temperatures are in a good agreement with experiment. The case of MnO is different because both NN and NNN couplings are antiferromagnetic and comparable in magnitude, for which the error in the estimated Neel temperature is larger, which is a signature of additional effects not captured by electronic structure calculations.

Simulating and designing novel antiferromagnetic materials (AFM) materials has been one of the main interests of solid-state chemistry, condensed matter, materials science, as well as engineering. AFM are of technological importance for designing spin valves, room-temperature electrical switches, colossal magnetoresistive effects, fast magnetic moment dynamics, and other antiferromagnetic spintronic applications.

The Neel temperature is the most important characteristic parameter describing AFM. It determines their technological applicability, since above the Neel temperature AFM undergoes a phase transition to a disordered phase from a phase where spins are displaying antiferromagnetic ordering. The theoretical determination of Neel temperature for realistic systems is very challenging due to several reasons. First, electronic structure of AFM is multiconfigurational and requires simultaneous treatment of both strong and weak electron correlation. Second, according to the Hohenberg–Mermin–Wagner theorem, magnetic critical phenomena can happen only in 3D bulk. Consequently, numerical simulations should be performed for periodic problems with taking into account possible finite-size effects. This requirement limits techniques such as exact diagonalization that are traditionally used for model Hamiltonians. Moreover, even for paradigmatic model systems such as 3D Hubbard model, a brute-force diagrammatic approach of evaluating finite-temperature susceptibilities gave unsatisfactory estimates of critical temperatures[1]. Not surprisingly, given the aforementioned challenges, there is a lack of rigorous quantum estimates of Neel temperatures for realistic AFM. For example, Neel temperatures of the transition-metal oxides studied in this work were estimated only with the techniques based on a classical Heisenberg model[2, 3] with somewhat ambiguously parametrized density functionals and a Hubbard U .

While using only model systems or brute-force realistic diagrammatic approaches have severe shortcomings, an alternative approach that is ab-initio and is based on quantum mechanics is still viable. In such an approach, effective exchange couplings present in the

quantum Heisenberg Hamiltonian can be extracted from DFT or wave-function calculations only using a limited number of computed states. These states are routinely accessible in standard electronic structure calculations. Subsequently, the constructed quantum Heisenberg Hamiltonian is extrapolated to encompass the states that cannot be efficiently captured by electronic structure calculations. Such a procedure is a very efficient way of computation of magnetic properties for molecular systems[4–8]. In the past, Pokhilko applied this extrapolation within equation-of-motion spin-flip coupled-cluster theory[9] not only for the states with low spin projections that cannot be captured, but also to the infinite system size, fully reproducing experimental magnetic susceptibility without any adjustable parameters[7].

Recently, we introduced a broken-symmetry GW approach [10, 11] based on the finite-temperature self-consistent GW code [12, 13] and benchmarked it for molecular systems and solids. In this work, we further extend the idea of using broken-symmetry GW to construct effective Hamiltonians according to the scheme below:

1. Extraction of magnetic couplings J from wave-function or broken-symmetry self-consistent periodic GW calculations and estimation of finite-size effects for J .
2. Evaluation of an extrapolated Heisenberg Hamiltonian for a large or even infinite system and reconstruction of the magnetic manifold of states of the target system.
3. Application of a high-temperature expansion (HTE) for spin susceptibilities and specific heat.
4. Determination of convergence radii of the expansions yielding the estimates of the Neel temperature.

We benchmark this approach on bulk NiO, CoO, FeO, and MnO against other theories and experiments.

Effective Hamiltonian. Magnetic phenomena can be accurately described with effective Hamiltonians since magnetic states are usually separated well from other states in the spectrum. In wave-function theories, such effective Hamiltonians can be constructed within the Bloch formalism as a result of an exact transformation from target to model spaces[4–7, 14–17]. However, in Green’s function or density-based methods, the wave-function amplitudes cannot be accessed directly and an alternative strategy has to be employed. This strategy relies on using broken-symmetry solutions possible to access in these methods. These Ising-like broken-symmetry solutions are found and their energies are used to extract magnetic couplings[18, 19]. In this paper to find these solutions, we use the fully self-consistent, finite-temperature GW approach starting from the unrestricted Hatree–Fock guess. The details of the broken-symmetry GW strategy can be found in Ref. [11].

For the metal oxides, we consider the following form of the the effective Hamiltonian established by previous broken-symmetry DFT calculations[2, 20–22]

$$H = -J_1 \sum_{\langle i,j \rangle} \vec{S}_i \vec{S}_j - J_2 \sum_{\langle\langle i,j \rangle\rangle} \vec{S}_i \vec{S}_j, \quad (1)$$

where $\langle i, j \rangle$ are the unique nearest-neighbor (NN) pairs, $\langle\langle i, j \rangle\rangle$ are the unique next-nearest-neighbor (NNN) pairs, J_1 is the NN effective exchange coupling, J_2 is the NNN effective exchange coupling, \vec{S}_i are the local (model) spins on metal center i . In all compounds studied in this work, the J_2 constant is antiferromagnetic. Therefore, all these oxides show

spin frustration that makes the determination of critical point especially difficult. To obtain exchange couplings, we use energy differences between the solutions with maximum and zero (broken-symmetry) spin projections evaluated using different unit cells. The exchange couplings are extracted according to the expressions below

$$J_{1,u} = -\frac{E(HS1) - E(BS1)}{16}, \quad (2)$$

$$J_{2,u} = -\frac{E(HS2) - E(BS2)}{12} - J_{1,u}, \quad (3)$$

where $E(\dots)$ denotes the energy of the high-spin (HS) and broken-symmetry (BS) solutions in cells 1 and 2 (see Ref. [11] for details).

In this work, we neglect relativistic effects since according to the Kanamori's estimate[23] the impact of the spin-orbit splitting in FeO and CoO on the Neel temperature is negligible. This is because the states, which as a result of spin-orbit coupling are non-degenerate, are fully thermally accessible. Our non-relativistic calculations when compared with experimental data will provide a good test of this prediction. While in this work, the impact of the relativistic effects on the Neel temperature is not significant, in general, the spin-orbit couplings between the degenerate non-relativistic states in Fe(II) and Co(II) are expected to be strong [23] and generalized in a more mathematically precise way by Pokhilko[24], resulting in spin-orbit splitting and single-ion anisotropy. This interplay of correlation and relativistic effects is of interest to both experimental and theory groups [25].

High-temperature expansion (HTE). HTE was introduced by Opechowski in 1937[26] and was subsequently applied to various Heisenberg and Ising Hamiltonians[27–32]. A prescription for a most general form of HTE for several coupling constants and arbitrary spin has only been introduced recently[33, 34]. The benefit of HTE is its applicability to highly frustrated systems. The main advantage of HTE is its a relatively low computational cost of evaluation of its coefficients. This allows one to study real space cells large enough to reach thermodynamic limit (TDL), thus eliminating the dependence of the final answer on the finite-size effects.

The idea of the HTE is the following. Thermodynamic quantities, such as spin susceptibility and specific heat, respectively, can be written as a Taylor series around $\beta = 0$

$$\chi = \sum_{n=0}^{\infty} c_n \beta^n, \quad (4)$$

$$C = \sum_{n=0}^{\infty} d_n \beta^n, \quad (5)$$

where β is the inverse temperature. We would like to note that in this work we neglect the orbital contribution to the magnetic susceptibility since its impact on the critical temperature is expected to be small. The first coefficient $c_0 = 0$, which gives the decay of χ to zero at an infinite temperature, corresponds to Curie law (c_1 defines the Curie constant). Critical temperature limits the radius of convergence of the series, since at the critical temperature the thermodynamic quantities are not analytic functions.

To find the critical temperature, the following ratios are commonly used

$$q_n = \left| \frac{c_n}{c_{n-1}} \right|, \quad (6)$$

$$s_n = \left| \frac{d_n}{d_{n-1}} \right|. \quad (7)$$

The q_n and s_n correspond to the d'Alembert test of convergence. At a large n , both q_n and s_n converge to the critical temperature. Another commonly used test is the root test based on $|c_n|^{1/n}$. However, each c_n is a homogeneous polynomial of degree $(n-1)$ of J_1 and J_2 . So the root estimate is unphysical because it is not strictly proportional to J . The ratios do not have this problem.

Instead of applying the root test to the χ , we apply the root test to $\frac{\chi}{\beta}$ or $\frac{\partial\chi}{\partial\beta}$:

$$g_n = |c_n|^{1/(n-1)} \rightarrow T_c, n \rightarrow \infty \quad (8)$$

$$h_n = |nc_n|^{1/(n-1)} \rightarrow T_c, n \rightarrow \infty \quad (9)$$

The g_n and h_n are proportional to J , which makes them more reliable.

At the same time, coefficients for the specific heat d_n are homogeneous polynomials of degree n of J_1 and J_2 .

$$f_n = |d_n|^{1/n} \rightarrow T_c, n \rightarrow \infty \quad (10)$$

$$r_n = |nd_n|^{1/n} \rightarrow T_c, n \rightarrow \infty \quad (11)$$

We applied all of the estimators described above, which we report in Section 3 in SI. We also tried various extrapolation techniques[35, 36], decomposition of $\log(\chi/\beta)$ and $\log(\chi')$, but the results were not satisfactory. Therefore, in this work, we limit our consideration to $q_n, s_n, g_n, h_n, f_n, r_n$.

Computational setup. We followed the computational protocol designed in Ref. [11] and used unit cells of different types to capture antiferromagnetic (broken-symmetry) solutions of different types. The used lattice constants are 4.1705Å [37], 4.4450Å [38], 4.2630Å [39], 4.285Å [40] for NiO, MnO, CoO, and FeO respectively. All calculations are performed with *gth-dzvp-molopt-sr* basis set[41], *gth-pbe* pseudopotential[42], *def2-svp-ri* auxiliary basis[43] for the resolution-of-identity decomposition, the Monkhorst-Pack k-point grid for the Brillouin-zone sampling[44] ($4 \times 4 \times 4$ for CoO and $5 \times 5 \times 5$ for FeO), Ewald approach[45, 46] for the treatment of the finite-size effects, and an intermediate representation[47] with $\Lambda = 10^5$ and 136 functions as a frequency grid. We used the one- and two-electron integrals computed with the PySCF code[48] to perform the GW calculations with the local in-house Green's function code [10, 12, 13, 49–51]. We used the frequency-dependent CDIIS algorithm[52] to accelerate the convergence of finite-temperature self-consistent GW iterations. For the high-temperature expansion, we wrote a program generating a spin graph with periodic boundary conditions for a cubic lattice and used it to construct a $20 \times 20 \times 20$ Hamiltonian from the Eq. 1. This Hamiltonian was then passed to the HTE10 code[34] generating expansions up to 10th order. We list the resulting expressions in SI in Section 2.

For the transition-metal oxides studied, Table I shows the effective exchange couplings J evaluated with rigorous ab-initio methods without any adjustable parameters. The broken-

TABLE I: The effective exchange couplings in K and their ratios employed in this work.

	NiO				MnO		
	J_1	J_2	J_2/J_1		J_1	J_2	J_2/J_1
Green's function methods							
UHF ^a	9.06	-57.77	-6.378	UHF ^a	-2.61	-2.09	0.800
GW ^a	18.95	-157.96	-8.335	GW ^a	-7.56	-6.70	0.887
Wave-function methods							
CASSCF ^b	5.80	-58.02	-10.00	CASSCF ^c	-31.9	–	
CASPT2 ^b	13.93	-193.80	-13.92	CASPT2 ^c	-95.0	–	
DDCI2 ^b	13.93	-146.22	-10.50				
DDCI3 ^b	20.89	-189.16	-9.056				
	CoO				FeO		
	J_1	J_2	J_2/J_1		J_1	J_2	J_2/J_1
Green's function methods							
UHF ^d	3.13	-11.42	-3.647	UHF ^d	3.64	-5.62	-1.545
GW ^d	3.30	-33.41	-10.12	GW ^d	3.83	-13.56	-3.540

^a: Reference[11]

^b: Reference[20]

^c: Reference[53]

^d: This work.

symmetry UHF and GW estimates for FeO and CoO evaluated in this work yield ferromagnetic J_1 and antiferromagnetic J_2 constants. For both NiO and MnO, similarly to FeO, GW increases the magnitude of J_2 in comparison to UHF. This can be explained by enhancement of the superexchange due to a partial stabilization of charge-transfer contributions because of the effective screened interaction W .

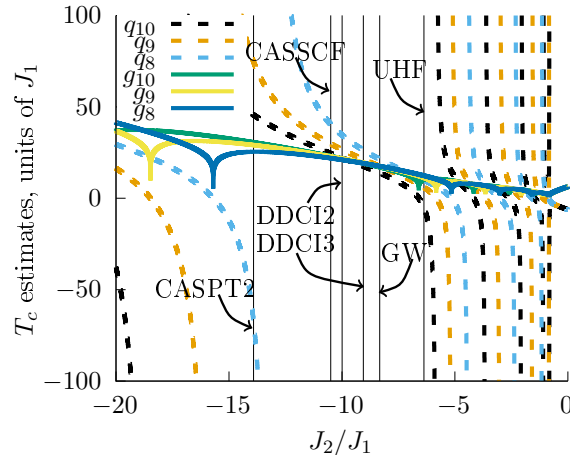


FIG. 1: Behavior of various estimates with respect to the J_2/J_1 ratios for NiO. The shown q_n ratios are signed to show the pole structure. Specific values of the J_2/J_1 ratios from quantum chemical calculations are marked with vertical lines. Neel temperature estimates can be seen as intersection points between the vertical lines and the ratio or root estimates.

We validate the high-temperature expansion by applying it to cubic lattices as described

in Section 1 in SI. There, we also provide a comparison of limiting cases with the previously published results from Refs[27, 30, 54, 55].

The Neel temperatures extracted from different convergence radius estimates can vary vastly. This behaviour is illustrated by Figure 1, which shows the dependence of q_n and g_n on the ratio of J_2 and J_1 constants for $S = 1$ case, corresponding to NiO. The q_n ratios change smoothly with J_2/J_1 for positive J_2/J_1 , but show multiple poles when J_2/J_1 is negative. The J_2/J_1 ratios computed with quantum chemical calculations lie in close proximity to the q_n poles resulting in a high sensitivity of q_n on the J_2/J_1 . The estimates based on the roots (Table S3 in SI) are much more stable and show a clear convergence pattern.

The behavior of the convergence radius estimates for CoO and FeO ($S = 3/2$ and $S = 2$) is similar to NiO. In SI, Tables S4 and S5 show the root estimates linking the Neel temperature and J_2 for a given J_2/J_1 values. An increase in S leads to higher T_N/J_2 values, which is expected from the form of the polynomials as explained in Refs[33, 34].

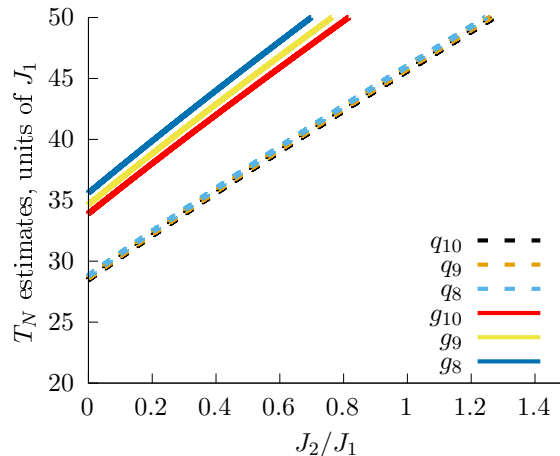


FIG. 2: Behavior of various estimates with respect to the J_2/J_1 ratios for MnO.

In SI, Tables S6 and S7 show the estimates for MnO. Since all the poles of q_n are located in the negative J_2/J_1 region, the positive J_2/J_1 provided by UHF and GW are far enough from the poles to stabilize the estimates based on q_n (Figure 2). Indeed, all q_n converge faster than the root estimates, leading to a good Domb–Sykes extrapolation (Table S1 in SI). The multiplication constants connecting the T_N and J_2 for MnO are much larger than for other compounds, which cannot be rationalized by the S values alone. Since the $J_2/J_1 \approx 1$, both NN and NNN are coupled with comparable constants, resulting in an effective coordination number equal to 18. In the mean-field treatment, the critical temperature is proportional to the coordination number. Early publications on high-temperature expansions[27, 30] preserved this trend and showed that the larger the coordination number is, the larger the multiplier is, which explains our findings.

Table II shows Neel temperatures extracted from the experimental measurements and evaluated from ab-initio calculations. For NiO, DDCI3 provides the most reliable estimate of J_1 , J_2 , and consequently the Neel temperature that is closest to experimental data. GW J_2/J_1 ratio is close to the DDCI3, which indicates that GW provides a balanced estimate of the effective exchange constants. GW improves the treatment of electronic correlation from UHF and provides estimates of the exchange constants close to DDCI2, which explains that a substantial part of dynamic electronic correlation in these compounds comes from

TABLE II: Estimates of Neel temperature (K) based on g_{10} and h_{10} , f_{10} and r_{10} .

Exp	NiO	CoO	FeO	MnO
	530 ^a , 516 ^b , 524.5 ^c , 523 ^d , 520 ^g	288 ^e , 293 ^g , 289.7 ^g	198 ^g , 183 ^g	118 ^f , 122 ^g , 116 ^g
UHF	94–121; 129–162	48–62; 53–66	36–46; 47–59	107 (q_∞); 100 (s_∞)
GW	324–419; 349–439	153–198; 144–181	70–90; 103–130	321 (q_∞); 299 (s_∞)
DDCI2	320–414; 320–403			
DDCI3	401–518; 416–524			
CASSCF	126–163; 127–160			
CASPT2	426–551; 419–528			

^a: Reference[56]

^b: Reference[57]

^c: Reference[58]

^d: Reference[59]

^e: Reference[60]

^f: Reference[61]

^g: Reference[62]

screening. Underestimation of the absolute values of the GW exchange constants result in an underestimation of the Neel temperature. All the GW root estimates reproduce the trend in the experimental estimates of Neel temperatures for NiO, CoO, and FeO. An agreement of FeO and CoO with this trend indicates that the spin-orbit interaction does not distort the structure of the magnetic Hamiltonian significantly to change the effective description from $S = 2$ and $S = 3/2$ to lower values, which is consistent with Kanamori's prediction[23]. This observation is contrary to Refs.[25, 63] where only the lower-lying manifold of spin-orbit-adiabatic states were considered for the effective magnetic Hamiltonian.

However, the MnO is different. Surprisingly, the UHF Neel temperature estimates are close to the experimental estimates for MnO, which is likely due to a fortuitous error cancellation. The GW increases the strengths of magnetic interactions and overestimates the Neel temperature in MnO. A plausible reason behind this disagreement is the existence of a structural phase transition from the low-temperature distorted structure to the high-temperature rock-salt structure. According to neutron diffraction experiments[59, 61], in NiO and FeO this structural transition happens at a much lower temperature than the magnetic phase transition. In MnO, the structural and magnetic phase transitions either happen together or separated only by ~ 1 K. In either case, one can expect substantial spin-vibronic effects[64], which are not taken into account in our calculations.

In this work, we applied broken-symmetry fully self-consistent GW approach and evaluated the effective exchange couplings in nickel, manganese, cobalt, and iron oxides. In both FeO and CoO, the J_1 constant is ferromagnetic and the J_2 constant is antiferromagnetic similar to NiO. The GW estimate of $|J_2|$ is several times larger than the UHF estimate. This observation is consistent with other solid and molecular compounds with significant superexchange, which can be explained by the inclusion of screened interactions in GW stabilising ionic contributions[10, 11]. The UHF and GW estimates of J_1 are similar, a possible explanation of which is in the dominance of the direct mechanism of exchange.

We found that when the signs of J_1 and J_2 are different, the q_n ratios contain multiple poles close to the computed J_1/J_2 values, making critical temperature estimates based on q_n unreliable in this regime. The estimates based on roots (g_n, h_n, f_n, r_n) are much more

stable and converge faster than q_n . The Neel temperature estimates derived from spin susceptibility and specific heat are in excellent agreement with each other. For NiO, the critical temperature evaluated from GW is in agreement with the estimates from the wavefunction calculations. The estimated critical temperatures from GW for NiO, CoO, and FeO reproduce the trend in the experimental estimates of critical temperature for this series of compounds.

If the signs of J_1 and J_2 are the same, the q_n are separated from the poles and become stable. This regime is observed for MnO, for which q_n converge faster than the root estimates. The Neel temperature of MnO is very sensitive to its J values, which can be explained by large spin ($S = 5/2$) and large effective coordination number. For MnO, the GW overestimates the critical temperature. While the precise cause of this overestimation is not known, plausible causes, such as spin-vibronic effects and deviation from Heisenberg Hamiltonian, will be investigated in our future work.

Acknowledgments

D.Z. and P.P. were supported by the Simons Foundation via the Simons Collaboration on the Many-Electron problem.

Supplementary Material

Validation, expressions for HTE coefficients, Neel temperature estimates.

-
- [1] S. Iskakov and E. Gull, Phase transitions in partial summation methods: Results from the three-dimensional Hubbard model, *Phys. Rev. B* **105**, 045109 (2022).
- [2] T. Archer, C. D. Pemmaraju, S. Sanvito, C. Franchini, J. He, A. Filippetti, P. Delugas, D. Puggioni, V. Fiorentini, R. Tiwari, and P. Majumdar, Exchange interactions and magnetic phases of transition metal oxides: Benchmarking advanced ab initio methods, *Phys. Rev. B* **84**, 115114 (2011).
- [3] X. Wan, Q. Yin, and S. Y. Savrasov, Calculation of magnetic exchange interactions in Mott-Hubbard systems, *Phys. Rev. Lett.* **97**, 266403 (2006).
- [4] N. J. Mayhall and M. Head-Gordon, Computational quantum chemistry for single Heisenberg spin couplings made simple: Just one spin flip required, *J. Chem. Phys.* **141**, 134111 (2014).
- [5] N. J. Mayhall and M. Head-Gordon, Computational quantum chemistry for multiple-site Heisenberg spin couplings made simple: Still only one spin-flip required, *J. Phys. Chem. Lett.* **6**, 1982 (2015).
- [6] P. Pokhilko and A. I. Krylov, Effective Hamiltonians derived from equation-of-motion coupled-cluster wave-functions: Theory and application to the Hubbard and Heisenberg Hamiltonians, *J. Chem. Phys.* **152**, 094108 (2020).
- [7] P. Pokhilko, D. S. Bezrukov, and A. I. Krylov, Is solid copper oxalate a spin chain or a mixture of entangled spin pairs?, *J. Phys. Chem. C* **125**, 7502 (2021).
- [8] S. Kotaru, S. Kähler, M. Alessio, and A. I. Krylov, Magnetic exchange interactions in binuclear and tetranuclear iron(III) complexes described by spin-flip DFT and Heisenberg effective Hamiltonians, *J. Comput. Chem.* **n/a**.
- [9] A. I. Krylov, Size-consistent wave functions for bond-breaking: The equation-of-motion spin-flip model, *Chem. Phys. Lett.* **338**, 375 (2001).
- [10] P. Pokhilko and D. Zgid, Interpretation of multiple solutions in fully iterative GF2 and GW schemes using local analysis of two-particle density matrices, *J. Chem. Phys.* **155**, 024101 (2021).
- [11] P. Pokhilko and D. Zgid, Broken-symmetry self-consistent GW approach: Degree of spin contamination and evaluation of effective exchange couplings in solid antiferromagnets, *J. Chem. Phys.* **157**, 144101 (2022).

- [12] S. Iskakov, C.-N. Yeh, E. Gull, and D. Zgid, Ab initio self-energy embedding for the photoemission spectra of NiO and MnO, *Phys. Rev. B* **102**, 085105 (2020).
- [13] C.-N. Yeh, S. Iskakov, D. Zgid, and E. Gull, Fully self-consistent finite-temperature GW in Gaussian Bloch orbitals for solids, arXiv , <https://arxiv.org/abs/2206.07660> (2022).
- [14] C. J. Calzado, J. Cabrero, J. P. Malrieu, and R. Caballol, Analysis of the magnetic coupling in binuclear complexes. II. Derivation of valence effective hamiltonians from ab initio CI and DFT calculations, *J. Chem. Phys.* **116**, 3985 (2002).
- [15] R. Maurice, R. Bastardis, C. de Graaf, N. Suaud, T. Mallah, and N. Guih ery, Universal theoretical approach to extract anisotropic spin hamiltonians, *J. Chem. Theory Comput.* **5**, 2977 (2009).
- [16] A. Monari, D. Maynau, and J.-P. Malrieu, Determination of spin Hamiltonians from projected single reference configuration interaction calculations. I. Spin 1/2 systems, *J. Chem. Phys.* **133**, 044106 (2010).
- [17] J. P. Malrieu, R. Caballol, C. J. Calzado, C. de Graaf, and N. Guih ery, Magnetic interactions in molecules and highly correlated materials: Physical content, analytical derivation, and rigorous extraction of magnetic Hamiltonians, *Chem. Rev.* **114**, 429 (2013).
- [18] L. Noodleman, Valence bond description of antiferromagnetic coupling in transition metal dimers, *J. Chem. Phys.* **74**, 5737 (1981).
- [19] K. Yamaguchi, Y. Takahara, and T. Fueno, Ab-initio molecular orbital studies of structure and reactivity of transition metal-oxo compounds, in *Applied quantum chemistry*, pages 155–184. Springer, 1986.
- [20] I. de P. R. Moreira, F. Illas, and R. L. Martin, Effect of Fock exchange on the electronic structure and magnetic coupling in NiO, *Phys. Rev. B* **65**, 155102 (2002).
- [21] X. Feng, Electronic structure of MnO and CoO from the B3LYP hybrid density functional method, *Phys. Rev. B* **69**, 155107 (2004).
- [22] C. Franchini, V. Bayer, R. Podloucky, J. Paier, and G. Kresse, Density functional theory study of MnO by a hybrid functional approach, *Phys. Rev. B* **72**, 045132 (2005).
- [23] J. Kanamori, Theory of the Magnetic Properties of Ferrous and Cobaltous Oxides, I, *Progr. Theor. Exp. Phys.* **17**, 177 (1957).
- [24] P. Pokhilko and A. I. Krylov, Quantitative El-Sayed rules for many-body wavefunctions from spinless transition density matrices, *J. Phys. Chem. Lett.* **10**, 4857 (2019).

- [25] P. M. Sarte, S. D. Wilson, J. P. Attfield, and C. Stock, Magnetic fluctuations and the spin-orbit interaction in Mott insulating CoO, *J. of Phys.: Cond. Matter* **32** (2020).
- [26] W. Opechowski, On the exchange interaction in magnetic crystals, *Physica* **4**, 181 (1937).
- [27] G. S. Rushbrooke and P. J. Wood, On the high-temperature susceptibility for the Heisenberg model of a ferromagnet, *Proc. Phys. Soc. A* **68**, 1161 (1955).
- [28] P. J. Wood and G. S. Rushbrooke, On the high temperature susceptibility for the heisenberg model of a ferromagnetic, *Proc. Phys. Soc. A* **70**, 765 (1957).
- [29] G. S. Rushbrooke and P. J. Wood, On the Curie points and high temperature susceptibilities of Heisenberg model ferromagnetics, *Mol. Phys.* **1**, 257 (1958).
- [30] C. Domb and M. F. Sykes, On the susceptibility of a ferromagnetic above the Curie point, *Proc. R. Soc. Lond. A* **240**, 214 (1957).
- [31] N. Elstner, R. R. P. Singh, and A. P. Young, Finite temperature properties of the spin-1/2 Heisenberg antiferromagnet on the triangular lattice, *Phys. Rev. Lett.* **71**, 1629 (1993).
- [32] N. Elstner and A. P. Young, Spin-1/2 Heisenberg antiferromagnet on the kagome lattice: High-temperature expansion and exact-diagonalization studies, *Phys. Rev. B* **50**, 6871 (1994).
- [33] H.-J. Schmidt, A. Lohmann, and J. Richter, Eighth-order high-temperature expansion for general Heisenberg Hamiltonians, *Phys. Rev. B* **84**, 104443 (2011).
- [34] A. Lohmann, H.-J. Schmidt, and J. Richter, Tenth-order high-temperature expansion for the susceptibility and the specific heat of spin- s Heisenberg models with arbitrary exchange patterns: Application to pyrochlore and kagome magnets, *Phys. Rev. B* **89**, 014415 (2014).
- [35] A. C. Aitken, Xxv.—on Bernoulli's numerical solution of algebraic equations, *Proc. Roy. Soc. Edinburgh* **46**, 289 (1927).
- [36] S. Lubkin, A method of summing infinite series, *J. Res. Nat. Bur. Standards* **48**, 228 (1952).
- [37] L. C. Bartel and B. Morosin, Exchange striction in NiO, *Phys. Rev. B* **3**, 1039 (1971).
- [38] W. D. Johnston and R. R. Heikes, A study of the $\text{Li}_x\text{Mn}_{(1-x)}\text{O}$ system, *J. Am. Chem. Soc.* **78**, 3255 (1956).
- [39] S. Sasaki, K. Fujino, and Y. Takeuchi, X-ray determination of electron-density distributions in oxides, MgO, MnO, CoO, and NiO, and atomic scattering factors of their constituent atoms, *Proc. Jpn. Acad. Ser. B* **55**, 43 (1979).
- [40] O. Crisan and A.D. Crisan, Phase transformation and exchange bias effects in mechanically alloyed Fe/magnetite powders, *J. Alloys Compd.* **509**, 6522 (2011).

- [41] J. VandeVondele and J. Hutter, Gaussian basis sets for accurate calculations on molecular systems in gas and condensed phases, *J. Chem. Phys.* **127**, 114105 (2007).
- [42] S. Goedecker, M. Teter, and J. Hutter, Separable dual-space Gaussian pseudopotentials, *Phys. Rev. B* **54**, 1703 (1996).
- [43] C. Hättig, Optimization of auxiliary basis sets for RI-MP2 and RI-CC2 calculations: Core-valence and quintuple- ζ basis sets for H to Ar and QZVPP basis sets for Li to Kr, *Phys. Chem. Chem. Phys.* **7**, 59 (2005).
- [44] H. J. Monkhorst and J. D. Pack, Special points for Brillouin-zone integrations, *Phys. Rev. B* **13**, 5188 (1976).
- [45] Joachim Paier, Robin Hirschl, Martijn Marsman, and Georg Kresse, The Perdew–Burke–Ernzerhof exchange-correlation functional applied to the G2-1 test set using a plane-wave basis set, *J. Chem. Phys.* **122**, 234102 (2005).
- [46] Ravishankar Sundararaman and T. A. Arias, Regularization of the Coulomb singularity in exact exchange by Wigner-Seitz truncated interactions: Towards chemical accuracy in nontrivial systems, *Phys. Rev. B* **87**, 165122 (2013).
- [47] H. Shinaoka, J. Otsuki, M. Ohzeki, and K. Yoshimi, Compressing Green’s function using intermediate representation between imaginary-time and real-frequency domains, *Phys. Rev. B* **96**, 035147 (2017).
- [48] Q. Sun, T. C. Berkelbach, N. S. Blunt, G. H. Booth, S. Guo, Z. Li, J. Liu, J. D. McClain, E. R. Sayfutyarova, S. Sharma, S. Wouters, and G. K. Chan, Pyscf: the python-based simulations of chemistry framework, *Wiley Interdiscip. Rev.: Comput. Mol. Sci.* **8**, e1340 (2017).
- [49] A. A. Rusakov and D. Zgid, Self-consistent second-order Green’s function perturbation theory for periodic systems, *J. Chem. Phys.* **144**, 054106 (2016).
- [50] P. Pokhilko, S. Isakov, C.-N. Yeh, and D. Zgid, Evaluation of two-particle properties within finite-temperature self-consistent one-particle Green’s function methods: Theory and application to GW and GF2, *J. Chem. Phys.* **155**, 024119 (2021).
- [51] C.-N. Yeh, A. Shee, Q. Sun, E. Gull, and D. Zgid, Relativistic self-consistent *gw*: Exact two-component formalism with one-electron approximation for solids, *Phys. Rev. B* **106**, 085121 (2022).
- [52] P. Pokhilko, C.-N. Yeh, and D. Zgid, Iterative subspace algorithms for finite-temperature solution of Dyson equation, *J. Chem. Phys.* **156**, 094101 (2022).

- [53] C. de Graaf, C. Sousa, I. de P. R. Moreira, and F. Illas, Multiconfigurational perturbation theory: An efficient tool to predict magnetic coupling parameters in biradicals, molecular complexes, and ionic insulators, *J. Phys. Chem. A* **105**, 11371 (2001).
- [54] M. Troyer, F. Alet, and S. Wessel, Histogram methods for quantum systems: from reweighting to Wang-Landau sampling, *Braz. J. Phys.* **34**, 377 (2004).
- [55] D. W. Wood and N. W. Dalton, Ferromagnetic Curie temperatures of the Heisenberg model with next-nearest-neighbor interactions, *Phys. Rev.* **159**, 384 (1967).
- [56] T. Chatterji, G. J. McIntyre, and P.-A. Lindgard, Antiferromagnetic phase transition and spin correlations in NiO, *Phys. Rev. B* **79**, 172403 (2009).
- [57] M. W. Vernon, The temperature dependence of the rhombohedral distortion in NiO, *Phys. Stat. Sol.* **37**, K1 (1970).
- [58] G. Srinivasan and M. S. Seehra, Magnetic susceptibilities, their temperature variation, and exchange constants of NiO, *Phys. Rev. B* **29**, 6295 (1984).
- [59] A. M. Balagurov, I. A. Bobrikov, S. V. Sumnikov, V. Yu. Yushankhai, and N. Mironova-Ulmane, Magnetostructural phase transitions in NiO and MnO: neutron diffraction data, *JETP Lett.* **104**, 88 (2016).
- [60] M. Massot, A. Oleaga, A. Salazar, D. Prabhakaran, M. Martin, P. Berthet, and G. Dhalenne, Critical behavior of CoO and NiO from specific heat, thermal conductivity, and thermal diffusivity measurements, *Phys. Rev. B* **77**, 134438 (2008).
- [61] A. P. Kantor, L. S. Dubrovinsky, N. A. Dubrovinskaia, I. Yu. Kantor, and I. N. Goncharenko, Phase transitions in MnO and FeO at low temperatures: A neutron powder diffraction study, *Journal of Alloys and Compounds* **402**, 42 (2005).
- [62] T. Nagamiya, K. Yosida, and R. Kubo, Antiferromagnetism, *Advances in Physics* **4**, 1 (1955).
- [63] V. Staemmler and K. Fink, An ab initio cluster study of the magnetic properties of the CoO(001) surface, *Chem. Phys.* **278**, 79 (2002).
- [64] D. J. Lockwood and M. G. Cottam, *Magnetic Interactions in the Cubic Mott Insulators NiO, MnO, and CoO and the Related Oxides CuO and FeO*, chapter 3, pages 51–73. John Wiley & Sons, Ltd, 2021.